Monatshefte für Chemie 132, 1463–1475 (2001)

Monatshefte für Chemie
Chemical Monthly

Study of the Ternary Systems M(II)$(NO_3)_2$–$LiNO_3$–H_2O (M(II) = Mg, Ca, Sr, Ba) at 25°C

Vladimír Zbranek* and **Jitka Eysseltová**

Department of Inorganic Chemistry, Faculty of Science, Charles University, CZ-12840 Prague, Czech Republic

Summary. The isothermal solubility diagrams of four aqueous systems containing lithium nitrate and nitrates of group IIA metals – magnesium, calcium, strontium, and barium – were studied at 25°C. No double salt formation was observed. The results were compared with similar nitrate and chloride systems. Some trends in the shape of the phase diagrams were observed. Hydration analysis was applied to the solubility branches, rendering information about ionic processes in saturated solutions. Further, the ratio of activity coefficients of the saturating solid phase in ternary and binary solutions (γ/γ_0) was obtained.

Keywords. Crystallization; Hydration analysis; Lithium nitrate; Solubility.

Introduction

Hydration analysis [1] was developed to yield information about ionic processes in saturated electrolyte solutions on the basis of computational analysis of solubility isotherms; it has been tested on systems consisting mainly of halogenides and sulfates. The most important value used during hydration analysis in these systems can be defined by

$$P = (w_0^{\mathrm{B}})_{\mathrm{changed}}/(M_{\mathrm{r}})_{\mathrm{H_2O}}\cdot(n_0^{\mathrm{B}} + n_1^{\mathrm{B}} + n_2^{\mathrm{B}}),$$

where

$$(w_0^{\mathrm{B}})_{\mathrm{changed}} = w_0^{\mathrm{B}} - \left((n_1^{\mathrm{B}})^{1/2}\cdot w_{0,1}^{\mathrm{A}}/n_1^{\mathrm{A}}\right)\cdot(n_1^{\mathrm{B}} + 2n_2^{\mathrm{B}})^{1/2}$$

when $LiNO_3$ is the saturating solid phase, and

$$(w_0^{\mathrm{B}})_{\mathrm{changed}} = w_0^{\mathrm{B}} - \left((n_1^{\mathrm{B}})^{1/3}\cdot w_{0,1}^{\mathrm{A}}/(2^{2/3}\cdot n_1^{\mathrm{A}})\right)\cdot(2n_1^{\mathrm{B}} + n_2^{\mathrm{B}})^{2/3}$$

for M(II)$(NO_3)_2$ as the saturating solid phase.

The superscripts A and B refer to the binary and ternary saturated solutions of the components, whereas the subscripts 1 and 2 indicate the saturating solid phase and the non-saturating component; the subscript 0 is used for water. $(M_r)_{H_2O}$ denotes the relative molecular weight of water, n_i is number of moles of the i-th

---

* Corresponding author. E-mail: jitka@natur.cuni.cz

component in 100 g of solution specified by the superscript, and $w_{0,1}^{\mathrm{A}}$ stands for the mass percent of water in the binary saturated solution of the respective saturating solid phase. The parameter P is equal to the amount of water which attains different properties in the three-component saturated solution than in a saturated binary solution [1]. For the sake of clarity, this parameter is usually expressed relative to one mole of the non-saturating component, *i.e.* P/x_1. The method was applied for the first time on systems where competitive hydration was the main process present [2] and, as a next step, on systems where complex formation occurs in saturated solutions [3].

Nitrate systems frequently exhibit quite high solubilities, being on the border line between aqueous solution and solution of water in salt melt. Thus, application of hydration analysis to such systems promised to yield interesting comparative information. Therefore, one aim of this work was to extend the application of hydration analysis to other groups of substances.

No reliable literature data were found for the series $M(NO_3)_2$–$LiNO_3$–H_2O, where M denotes an alkaline earth metal, with the only exception of the $Be(NO_3)_2$–$LiNO_3$–H_2O system which has been studied by *Balashova* and *Protsenko* at 25°C [4]. The $Mg(NO_3)_2$–$LiNO_3$–H_2O system has been investigated by *Chernykh et al.* [5] at 0 and 50°C simultaneously with our solubility studies of this system at 25°C.

Results and Discussion

The solubility isotherms in the systems investigated (Tables 1–4, Figs. 1–4) can be classified as simple eutonic at 25°C, except for the $Ca(NO_3)_2$–$LiNO_3$–H_2O system (Fig. 2) where this property cannot be identified.

These systems were studied for the first time except for $Mg(NO_3)_2$–$LiNO_3$–H_2O which can be compared with the work of *Chernykh et al.* [5] (Fig. 5). The system is eutonic at all temperatures under consideration. The shapes of the solubility isotherms and the positions of the eutonic points are similar, the crystallization branches of both components being of comparable length.

The solubility isotherm in the $Ca(NO_3)_2$–$LiNO_3$–H_2O system (Fig. 2) contains a relatively large region without a solid phase (*de facto* a melt). In the similar $Ca(NO_3)_2$–$Be(NO_3)_2$–H_2O [6] and $CaCl_2$–$LiCl$–H_2O [7, 8] systems the existence of lower hydrates of calcium salts – $Ca(NO_3)_2 \cdot 3H_2O$ and $CaCl_2 \cdot 3H_2O$, respectively – can be observed. Therefore we can assume with a high level of probability the existence of a lower hydrate in this melting region as well. This idea seems to be supported also by computer simulations using the BET model performed at the *TU Bergakademie Freiberg* [9, 10].

The shape of the solubility isotherm in the $Ba(NO_3)_2$–$LiNO_3$–H_2O system (Fig. 4) is quite unusual. Extremely high salting-out of barium nitrate occurs along the entire solubility branch. A very similar shaped solubility diagram can be found in the $Ba(NO_3)_2$–$Be(NO_3)_2$–H_2O system at 25°C [11].

Therefore, based on our measurements, the hydration analysis was performed for following crystallization branches: *i*) $Mg(NO_3)_2 \cdot 6H_2O$ in solution of lithium nitrate (Fig. 7), *ii*) $LiNO_3 \cdot 3H_2O$ in solution of magnesium nitrate (Fig. 8), *iii*) $Ca(NO_3)_2 \cdot 4H_2O$ in solution of lithium nitrate (Fig. 9), *iv*) $LINO_3 \cdot 3H_2O$ in

Table 1. Liquid phase composition (in mass %) in the $Mg(NO_3)_2$–$LiNO_3$–H_2O system at 25°C

$LiNO_3$	$Mg(NO_3)_2$	H_2O	Solid phase
46.55	–	53.45	$LiNO_3 \cdot 3H_2O$
40.40	6.94	52.66	$LiNO_3 \cdot 3H_2O$
39.00	9.07	51.94	$LiNO_3 \cdot 3H_2O$
36.93	12.15	50.92	$LiNO_3 \cdot 3H_2O$
34.87	15.44	49.69	$LiNO_3 \cdot 3H_2O$
33.89	16.56	49.55	$LiNO_3 \cdot 3H_2O$
33.47	17.74	48.79	$LiNO_3 \cdot 3H_2O$
32.86	18.95	48.19	$LiNO_3 \cdot 3H_2O + Mg(NO_3)_2 \cdot 6H_2O$
31.91	19.70	48.39	$Mg(NO_3)_2 \cdot 6H_2O$
28.64	21.40	49.97	$Mg(NO_3)_2 \cdot 6H_2O$
28.23	21.66	50.11	$Mg(NO_3)_2 \cdot 6H_2O$
25.71	22.95	51.34	$Mg(NO_3)_2 \cdot 6H_2O$
23.64	24.29	52.08	$Mg(NO_3)_2 \cdot 6H_2O$
22.73	25.01	52.26	$Mg(NO_3)_2 \cdot 6H_2O$
21.82	25.78	52.40	$Mg(NO_3)_2 \cdot 6H_2O$
21.84	25.66	52.50	$Mg(NO_3)_2 \cdot 6H_2O$
15.71	28.80	55.50	$Mg(NO_3)_2 \cdot 6H_2O$
11.29	32.60	56.11	$Mg(NO_3)_2 \cdot 6H_2O$
7.68	35.15	57.17	$Mg(NO_3)_2 \cdot 6H_2O$
2.41	39.04	58.55	$Mg(NO_3)_2 \cdot 6H_2O$
–	41.81	58.19	$Mg(NO_3)_2 \cdot 6H_2O$

Table 2. Liquid phase composition (in mass %) in the $Ca(NO_3)_2$–$LiNO_3$–H_2O system at 25°C

$LiNO_3$	$Ca(NO_3)_2$	H_2O	Solid phase
46.60	–	53.40	$LiNO_3 \cdot 3H_2O$
44.58	3.90	51.52	$LiNO_3 \cdot 3H_2O$
40.74	10.46	48.80	$LiNO_3 \cdot 3H_2O$
40.09	11.86	48.05	$LiNO_3 \cdot 3H_2O$
38.76	14.86	46.38	$LiNO_3 \cdot 3H_2O$
38.90	23.13	37.97	$LiNO_3 \cdot 3H_2O$
37.97	23.55	38.48	$LiNO_3 \cdot 3H_2O$
38.45	23.56	37.99	$LiNO_3 \cdot 3H_2O$
18.48	45.23	36.29	$Ca(NO_3)_2 \cdot 4H_2O$
16.87	45.15	37.98	$Ca(NO_3)_2 \cdot 4H_2O$
10.09	49.28	40.63	$Ca(NO_3)_2 \cdot 4H_2O$
4.29	53.69	42.02	$Ca(NO_3)_2 \cdot 4H_2O$
–	58.24	41.76	$Ca(NO_3)_2 \cdot 4H_2O$

solution of calcium nitrate (Fig. 10), and *v*) $Sr(NO_3)_2$ in solution of lithium nitrate (Fig. 11).

Moreover, a hydration analysis of the $Be(NO_3)_2$–$LiNO_3$–H_2O [4] system was performed (Figs. 12–13) to allow for a comparison in the complete group IIA. As far as the $Ba(NO_3)_2$–$LiNO_3$–H_2O system is concerned, it is not suitable for

Table 3. Liquid phase composition (in mass %) in the $Sr(NO_3)_2$–$LiNO_3$–H_2O system at 25°C

$LiNO_3$	$Sr(NO_3)_2$	H_2O	Solid phase
46.56	–	53.44	$LiNO_3 \cdot 3H_2O$
46.02	2.17	51.81	$LiNO_3 \cdot 3H_2O$
45.14	2.54	52.32	$LiNO_3 \cdot 3H_2O + Sr(NO_3)_2$
45.07	2.43	52.50	$LiNO_3 \cdot 3H_2O + Sr(NO_3)_2$
44.95	2.67	52.38	$LiNO_3 \cdot 3H_2O + Sr(NO_3)_2$
44.76	3.00	52.24	$LiNO_3 \cdot 3H_2O + Sr(NO_3)_2$
44.65	2.88	52.47	$LiNO_3 \cdot 3H_2O + Sr(NO_3)_2$
39.12	4.50	56.38	$Sr(NO_3)_2$
36.89	5.58	57.53	$Sr(NO_3)_2$
27.90	10.91	61.19	$Sr(NO_3)_2$
18.92	20.00	61.08	$Sr(NO_3)_2$
11.57	29.18	59.25	$Sr(NO_3)_2$
5.48	38.07	56.45	$Sr(NO_3)_2$
–	47.07	52.93	$Sr(NO_3)_2$

Table 4. Liquid phase composition (in mass %) in the $Ba(NO_3)_2$–$LiNO_3$–H_2O system at 25°C

$LiNO_3$	$Ba(NO_3)_2$	H_2O	Solid phase
46.56	–	53.44	$LiNO_3 \cdot 3H_2O$
46.37	0.43	53.20	$LiNO_3 \cdot 3H_2O + Ba(NO_3)_2$
46.34	0.44	53.22	$LiNO_3 \cdot 3H_2O + Ba(NO_3)_2$
46.29	0.41	53.30	$LiNO_3 \cdot 3H_2O + Ba(NO_3)_2$
46.12	0.47	53.41	$LiNO_3 \cdot 3H_2O + Ba(NO_3)_2$
42.47	0.44	57.09	$Ba(NO_3)_2$
25.93	0.59	73.48	$Ba(NO_3)_2$
16.46	1.00	82.54	$Ba(NO_3)_2$
9.85	1.81	88.34	$Ba(NO_3)_2$
6.45	2.95	90.61	$Ba(NO_3)_2$
3.15	5.28	91.58	$Ba(NO_3)_2$
0.74	8.34	90.92	$Ba(NO_3)_2$
–	9.27	90.73	$Ba(NO_3)_2$

hydration analysis. The above method treats the added ion as a disturbance in the structure of the binary solution, whereas along the entire crystallization branch of barium nitrate the content of barium is very strongly depressed, and the nature of this solution is very different from a binary saturated solution of barium nitrate. Besides, the solubility branch of $LiNO_3 \cdot 3H_2O$ in the $Sr(NO_3)_2$–$LiNO_3$–H_2O system is too short for applying the method according to the criteria stated in Ref. [12].

In Figs. 7–13, P/x_1 and the total amount of water available per ion of salt components (Aq) are plotted against the molality of added component in the liquid phase m_1. As demonstrated in Ref. [2], the hydration analysis yields also the ratio γ/γ_0, where γ and γ_0 are the activity coefficients of the solute in the ternary saturated

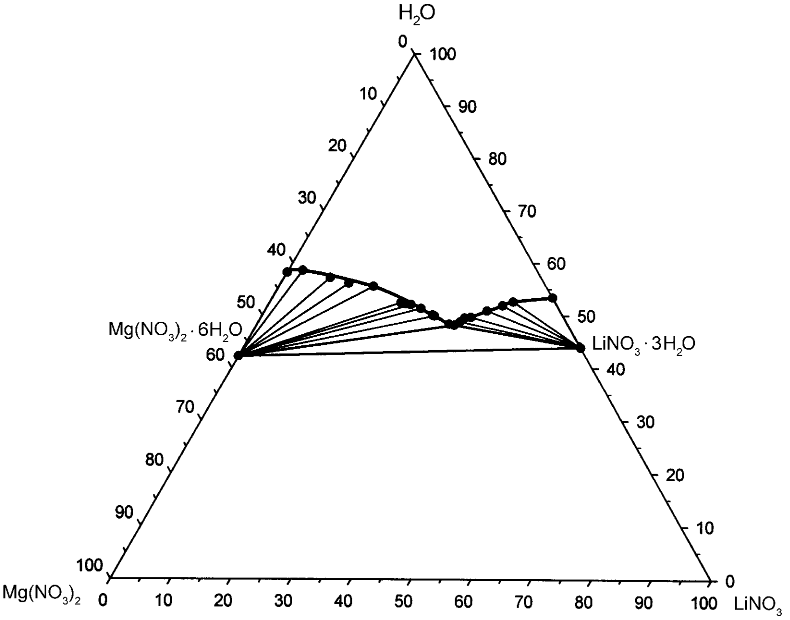

Fig. 1. Solubility diagram of the $Mg(NO_3)_2$–$LiNO_3$–H_2O system at 25°C

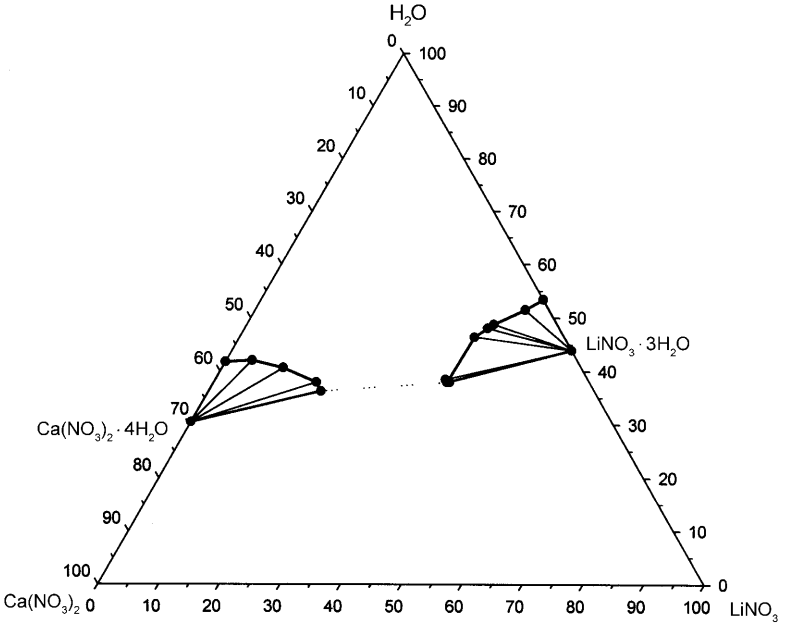

Fig. 2. Solubility diagram of the $Ca(NO_3)_2$–$LiNO_3$–H_2O system at 25°C

solution and in its saturated solution in water under the same conditions. In the systems under consideration, this ratio was also plotted against the molality of added component in liquid phase m_1 (Figs. 14 and 15).

Generally, we can state that the addition of the lithium cation has a very different effect in the various systems, and no smooth change is observable. This

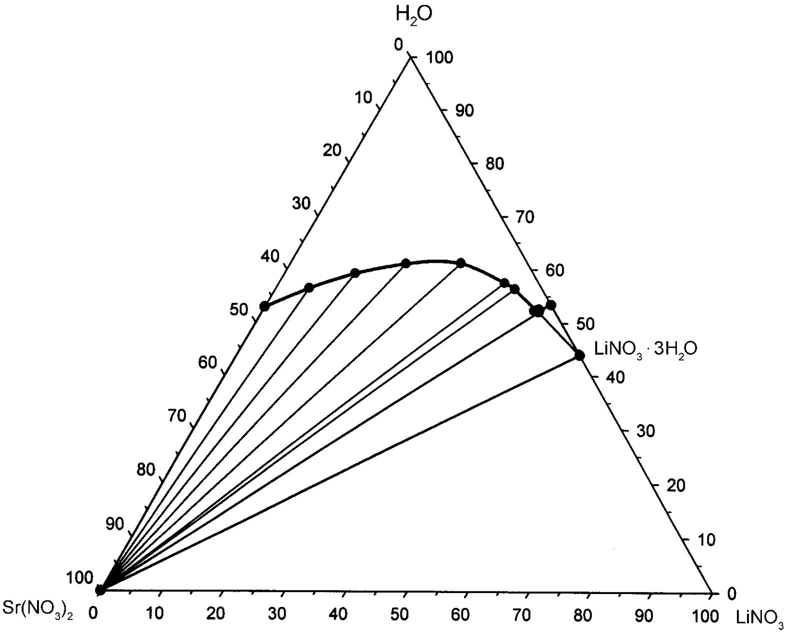

Fig. 3. Solubility diagram of the $Sr(NO_3)_2$–$LiNO_3$–H_2O system at 25°C

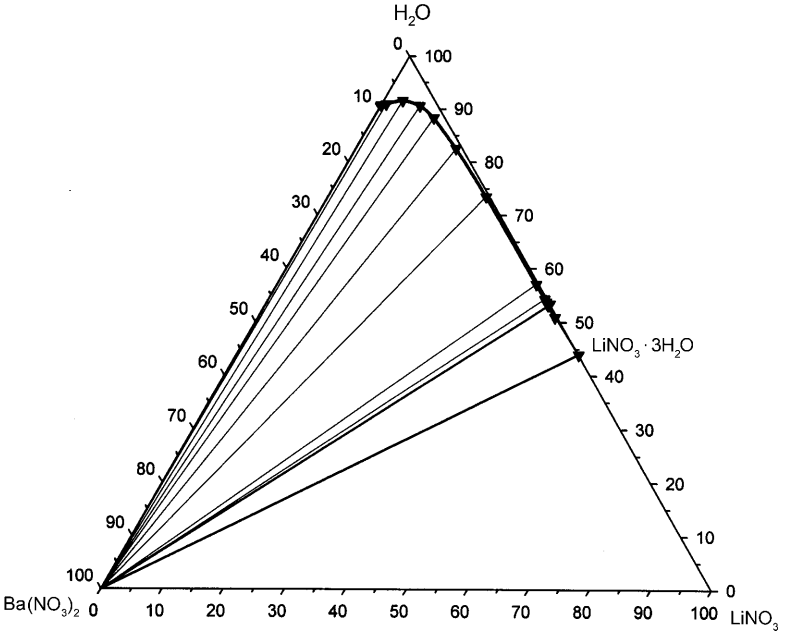

Fig. 4. Solubility diagram of the $Ba(NO_3)_2$–$LiNO_3$–H_2O system at 25°C

statement is valid both for the shape of the solubility diagram itself and for the results of hydration analysis.

In the $Be(NO_3)_2$–$LiNO_3$–H_2O system (Figs. 6, 12–13) studied by *Balashova* and *Protsenko* [4], three crystallization fields can be found. Strong salting-out of $LiNO_3 \cdot 3H_2O$ is observed in the neighborhood of anhydrous lithium nitrate. This

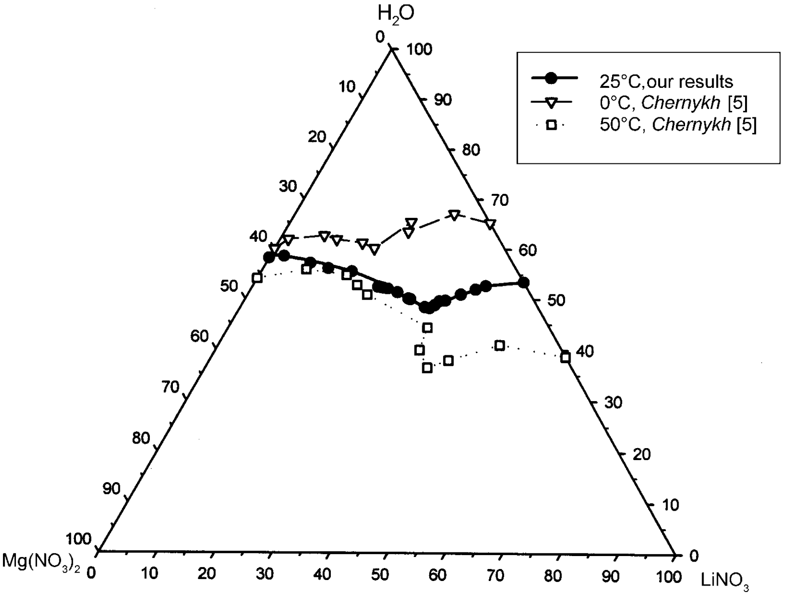

Fig. 5. Comparison of the solubility in the $Mg(NO_3)_2$–$LiNO_3$–H_2O system at 0, 25, and 50°C

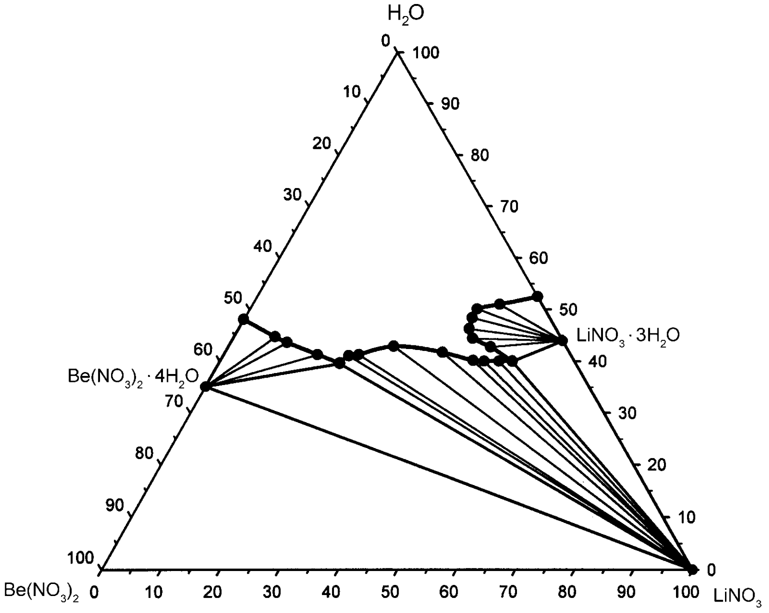

Fig. 6. Solubility diagram of the $Be(NO_3)_2$–$LiNO_3$–H_2O system at 25°C [4]

is the only system of this group in which dehydration of $LiNO_3 \cdot 3H_2O$ resulting in the field of anhydrous lithium nitrate was found. However, hydration analysis is applicable only on branches of the hydrates stable in binary systems, *i.e.* the parameter P is negative for both of these branches.

The hydration analysis of the crystallization branches of the nitrates of bivalent metals (Figs. 7, 9, 11–12) complies with mere competition for water molecules in

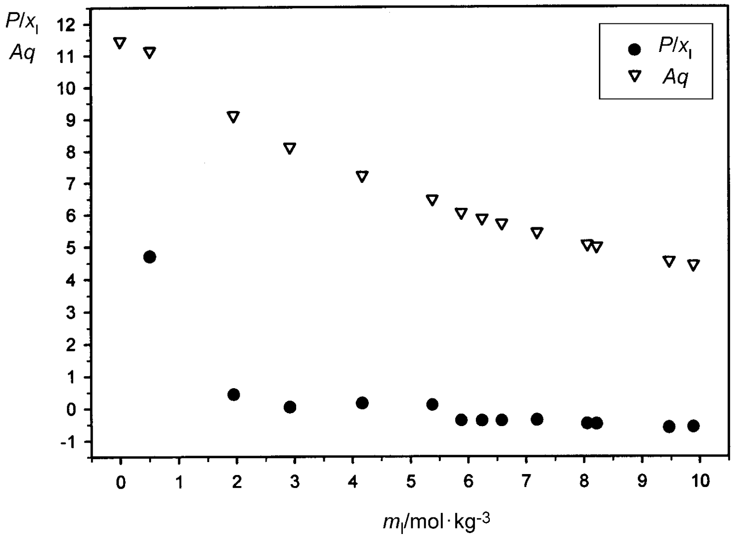

Fig. 7. Hydration analysis in the $Mg(NO_3)_2$–$LiNO_3$–H_2O system at 25°C (the saturating solid phase is $Mg(NO_3)_2 \cdot 6H_2O$); *Aq* denotes number of moles of water being at disposal per ion of salt component in the saturated solution

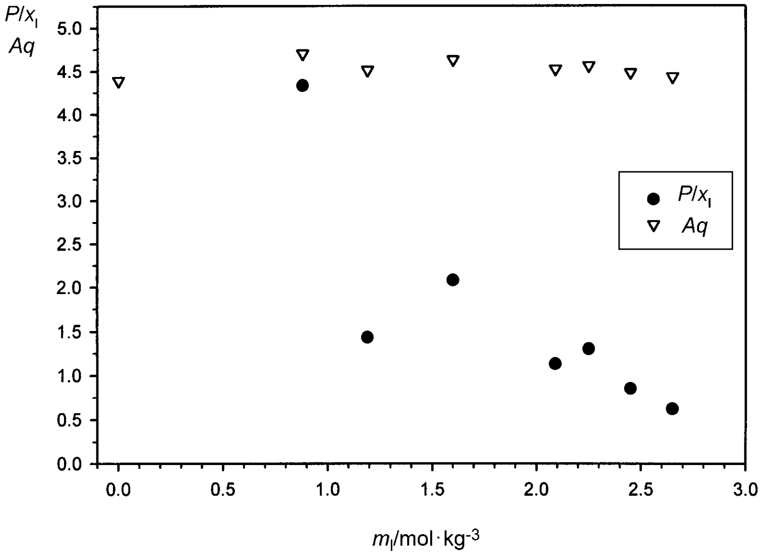

Fig. 8. Hydration analysis in the $Mg(NO_3)_2$–$LiNO_3$–H_2O system at 25°C (the saturating solid phase is $LiNO_3 \cdot 3H_2O$)

the case of beryllium and magnesium and the stepwise increase of association between *M*(II) and nitrate ions from beryllium to strontium. This ion association may be secondarily supported also by a reasonable reduction of the amount of water being at the disposal in concentrated solutions close to the eutonic composition. Otherwise, this shortage on water molecules induced no special features to the results of hydration analysis. On the other hand, the shape of the solubility

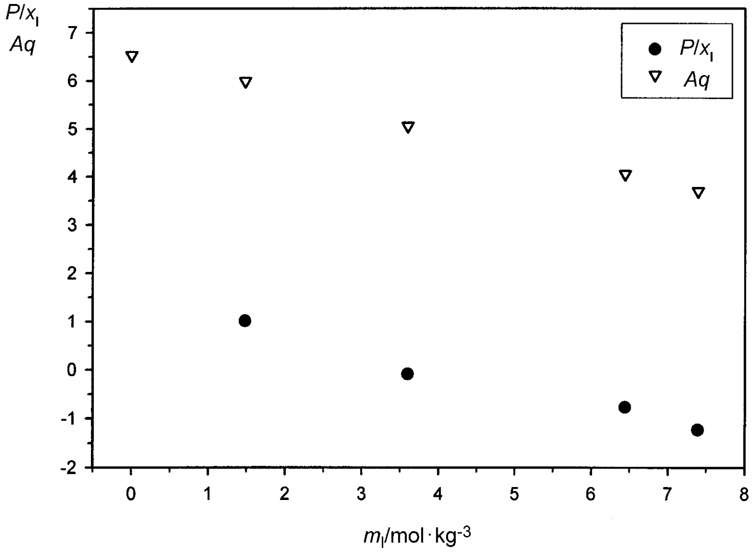

Fig. 9. Hydration analysis in the $Ca(NO_3)_2$–$LiNO_3$–H_2O system at 25°C (the saturating solid phase is $Ca(NO_3)_2 \cdot 4H_2O$)

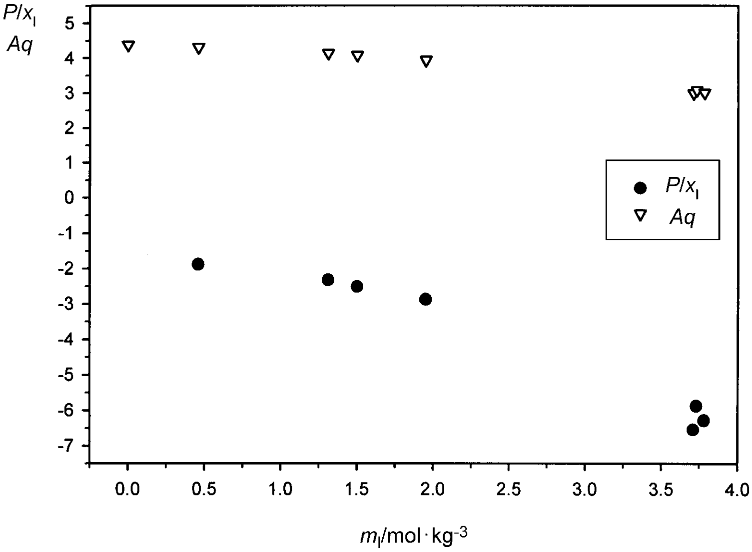

Fig. 10. Hydration analysis in the $Ca(NO_3)_2$–$LiNO_3$–H_2O system at 25°C (the saturating solid phase is $LiNO_3 \cdot 3H_2O$)

isotherms in this family of systems itself has inspired general discussion of the organization of saturated solutions of salt hydrates [13].

In a saturated solution of $LiNO_3 \cdot 3H_2O$ (Fig. 8), the addition of $Mg(NO_3)_2$ causes reorganization of the solution resulting in hydration of the Mg^{2+} ions added. The lack of water molecules seems to support the association of the present cations and nitrate ions, which is the main effect in the system with $Ca(NO_3)_2$ (Fig. 10).

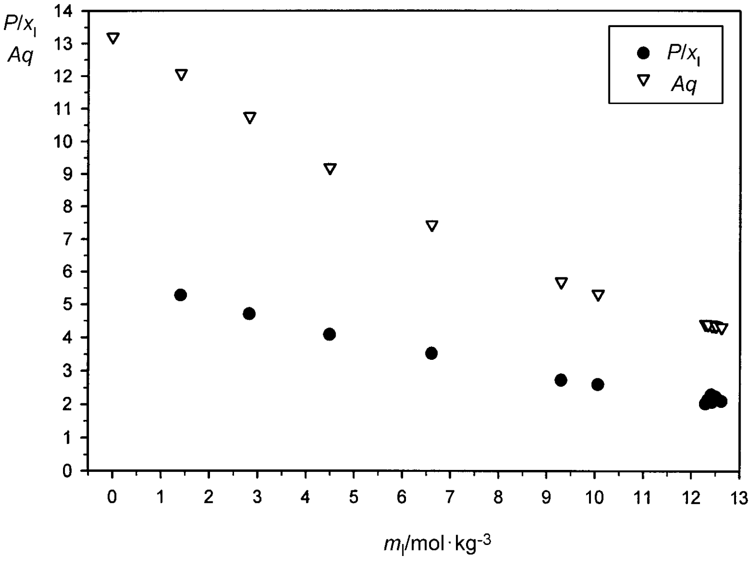

Fig. 11. Hydration analysis in the $Sr(NO_3)_2$–$LiNO_3$–H_2O system at 25°C (the saturating solid phase is $Sr(NO_3)_2$)

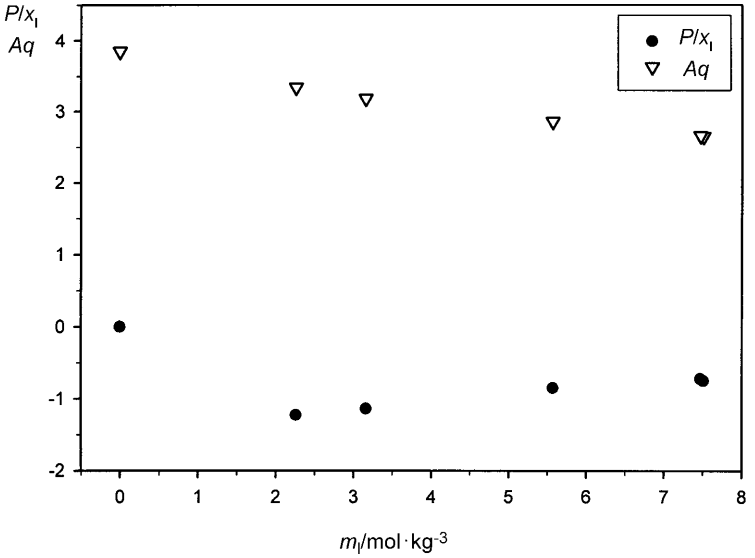

Fig. 12. Hydration analysis in the $Be(NO_3)_2$–$LiNO_3$–H_2O system at 25°C (the saturating solid phase is $Be(NO_3)_2 \cdot 4H_2O$)

Hydration analysis of the solubility of $LiNO_3{\cdot}3H_2O$ in solutions of $Be(NO_3)_2$ (Fig. 13) is in many features unique, even when compared with other systems exhibiting remarkable salting-in [14, 15]. It is only in the case of an addition of nitric acid to a saturated solution of $Mg(NO_3)_2 \cdot 6H_2O$ at 25°C [16] that such a retrograde effect can be observed in the results of hydration analysis as well. A more detailed investigation of this phenomenon is beyond the scope of this article. With highest probability, the Be^{2+} ion causes fundamental reorganization of the

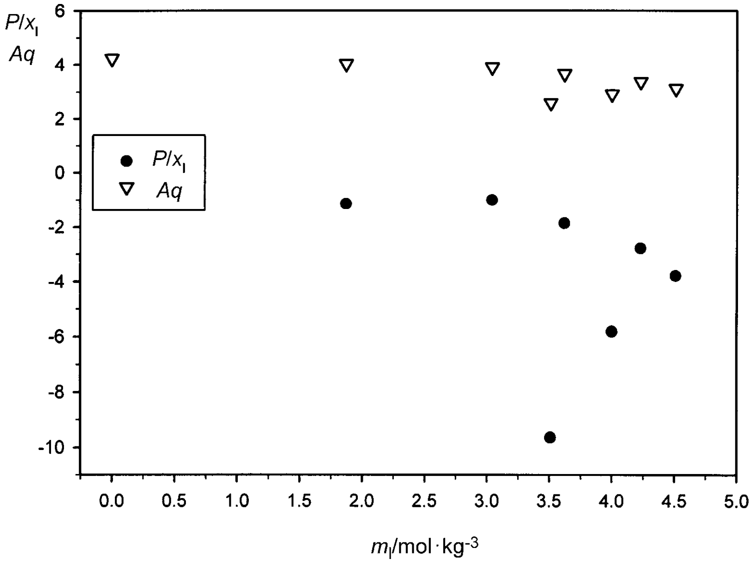

Fig. 13. Hydration analysis in the $Be(NO_3)_2$–$LiNO_3$–H_2O system at 25°C (the saturating solid phase is $LiNO_3 \cdot 3H_2O$)

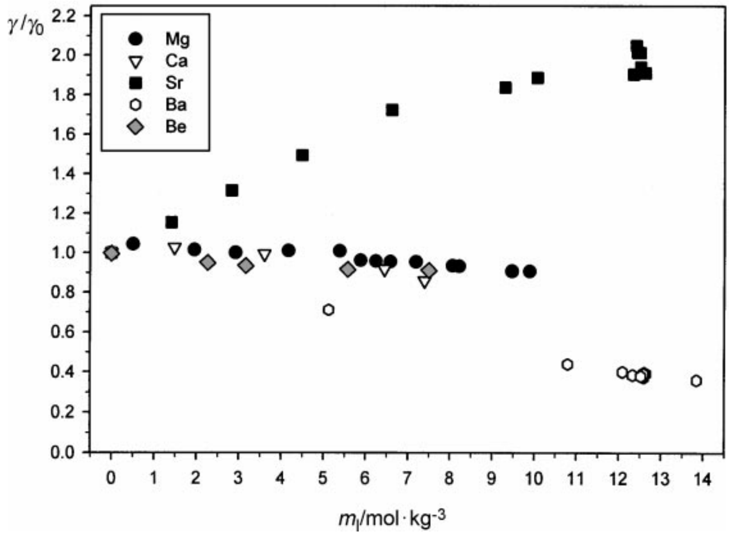

Fig. 14. Activity coefficients of $M(NO_3)_2$ in the $M(NO_3)_2$–$LiNO_3$–H_2O system (M = Be, Mg, Ca, Sr, Ba) at 25°C

saturated solution of $LiNO_3 \cdot 3H_2O$, which exhibits a strong degree of organization itself.

As a result, a strong hydration ability of the lithium cation has been observed in all title systems. No special features caused by high solubility were found. Mutual comparison of the shape of the solubility isotherms has inspired general discussion on the organization of saturated solutions of salt hydrates [13].

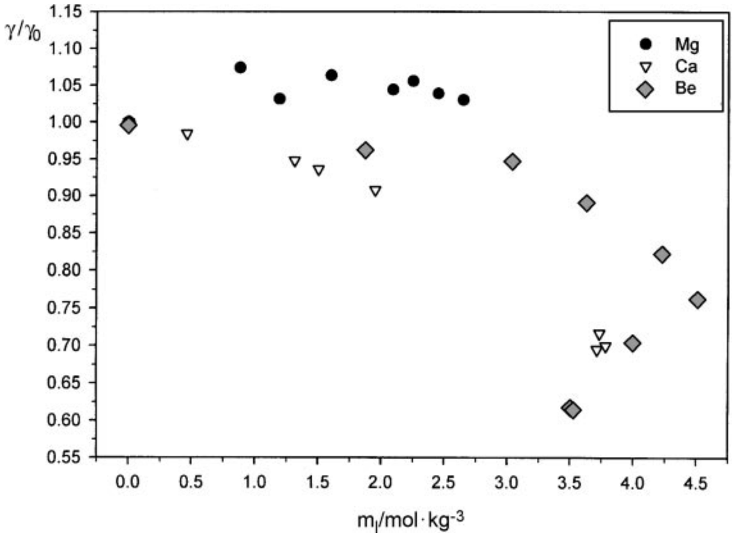

Fig. 15. Activity coefficients of $LiNO_3$ in the $M(NO_3)_2$–$LiNO_3$–H_2O system (M = Be, Mg, Ca) at 25°C

Experimental

Reagent grade chemicals ($LiNO_3$, $Mg(NO_3)_2 \cdot 6H_2O$, $Ca(NO_3)_2 \cdot 4H_2O$, $Sr(NO_3)_2$ from Lachema Brno; $Ba(NO_3)_2$ from VEB Laborchemie Apolda, former GDR) were used. Twenty phase complexes were prepared for each system and equilibrated in polyethylene or glass vessels placed in an air thermostat for approximately two months. The vessels were shaken on a mechanic shaking machine during the first two weeks. The temperature was kept constant within 25±0.2°C. The equilibrium was checked by complexometric determination of bivalent metal content of the saturated solutions.

After equilibration, part of the liquid phase was sampled with a pipette into a preweighed glass vessel and dried to constant weight at *ca*. 200°C to determine the content of water. Another part of the liquid phase was sampled and diluted to 50 cm^3. Bivalent metal contents in saturated solutions were determined complexometrically (Chelaton III). The content of lithium was calculated as the difference.

For the calculations of hydration analysis, an universal computational program (HYDRAN) was developed (Microsoft Visual Basic Version 5.0) [17]. Solubility diagrams and other graphs were created using the SPSS Sigma Plot program (Version 4.01).

Acknowledgements

The authors are indebted to *em*. Prof. RNDr. *Miroslav Ebert*, DrSc. for inspiring discussions.

References

[1] Eysseltová J (1994) Collect Czech Chem Commun **59**: 126
[2] Eysseltová J (1994) Collect Czech Chem Commun **59**: 2351
[3] Eysseltová J, Zbranek V, Jirsák J (1999) Collect Czech Chem Commun **64**: 1262
[4] Balashova EF, Protsenko PI (1970) Izv Vyssh Ucheb Zaved, Khim Khim Tekhnol **13**: 1109
[5] Chernykh LB, Bulgakova TN, Skripkin MYu, Burkov KA (1998) Zh Prikl Khim **71**: 1425
[6] Balashova EF, Protsenko PI (1970) Geterogen Ravnovesiya Nitritn Nitratn Sist. Rostovskij Gos Un-t, Elista, p 51

[7] Blidin VP (1952) Dokl Ak Nauk SSSR **84**: 947
[8] Blidin VP (1954) Issled Ak Nauk SSSR Khim **3**: 400
[9] Voigt W (1993) Monatsh Chem **124**: 349
[10] Voigt W, Zeng D (private communication)
[11] Balashova EF, Protsenko PI (1970) Geterogen Ravnovesiya Nitritn Nitratn Sist. Rostovskij Gos Un-t, Elista, p 55
[12] Eysseltová J (2001) Collect Czech Chem Commun **66**: 89
[13] Eysseltová J, Ebert M, Zbranek V (to be published)
[14] Balashova EF, Protsenko PI (1970) Geterogen Ravnovesiya Nitritn Nitratn Sist. Rostovskij Gos Un-t, Elista, p 33
[15] Balashova EF, Protsenko PI (1970) Geterogen Ravnovesiya Nitritn Nitratn Sist. Rostovskij Gos Un-t, Elista, p 41
[16] Ewing WW, Klinger E (1933) J Am Chem Soc **55**: 4825; (1969) In: Spravochnik po rastvorimosti. Nauka, Leningrad, p 206
[17] Zbranek V, Eysseltová J (1999) Proc Progr in Computing of Physicochemical Properties. Warszaw, Poland

Received April 13, 2001. Accepted June 15, 2001